

## Article

# Tribo-Catalytic Degradation of Methyl Orange Solutions Enhanced by Silicon Single Crystals

Xiaodong Cui <sup>1</sup>, Zhiyu Guo <sup>1,2</sup>, Hua Lei <sup>1</sup>, Xuchao Jia <sup>1</sup>, Chenyue Mao <sup>1</sup>, Lujie Ruan <sup>3,4</sup>, Xiaoyuan Zhou <sup>3,4</sup>, Zhu Wang <sup>5</sup>, Feng Chen <sup>6</sup> and Wanping Chen <sup>1,\*</sup>

<sup>1</sup> Key Laboratory of Artificial Micro- and Nano-Structures of Ministry of Education, School of Physics and Technology, Wuhan University, Wuhan 430072, China; xiaodongcui@whu.edu.cn (X.C.); christinaguo109@gmail.com (Z.G.); hualei@whu.edu.cn (H.L.); jiaxuchao@whu.edu.cn (X.J.); maochenyue1@163.com (C.M.)

<sup>2</sup> Department of Chemistry, University College London, London WC1H 0AJ, UK

<sup>3</sup> College of Physics, Chongqing University, Chongqing 401331, China; lujie\_ruan@foxmail.com (L.R.); xiaoyuan2013@cqu.edu.cn (X.Z.)

<sup>4</sup> Center of Quantum Materials and Devices, Chongqing University, Chongqing 401331, China

<sup>5</sup> Hubei Key Laboratory of Radiation Chemistry and Functional Materials, School of Nuclear Technology and Chemistry and Biology, Hubei University of Science and Technology, Xianning 437100, China; wangz@whu.edu.cn

<sup>6</sup> Guangdong Provincial Key Laboratory of Metal Toughening Technology and Application, Institute of New Materials, Guangdong Academy of Sciences, Guangzhou 510650, China; chenfang@gdinm.com

\* Correspondence: wpchen@whu.edu.cn

**Abstract:** Coating materials on the bottoms of reactors/beakers has emerged as an effective method to regulate tribo-catalytic reactions. In this study, silicon single crystals were coated on the bottoms of glass beakers, in which 30 mg/L methyl orange (MO) solutions suspended with alumina nanoparticles were subjected to magnetic stirring using Teflon magnetic rotary disks. With a gentle rotating speed of 400 rpm for the Teflon disks, the MO solutions were changed from yellow to colorless and the characteristic absorption peak of MO at 450 nm in the UV-Vis spectrum disappeared entirely within 120 min. Mass spectrometry tests were further performed to gain insights into the degradation process, which suggested that the degradation was initiated with the cleavage of the nitrogen-nitrogen double bond in ionized MO molecules by the attack of •OH radicals. Through comparison experiments, we established that the observed degradation was related to the friction between alumina and silicon during magnetic stirring, and hydroxyl and superoxide radicals were formed from the friction, according to electron paramagnetic resonance analysis. It is proposed that electron-hole pairs are excited in silicon single crystals through friction with alumina, which diffuse to the surface of the single crystals and result in the degradation.

**Keywords:** tribo-catalysis; silicon; coating; dye degradation; methyl orange



**Citation:** Cui, X.; Guo, Z.; Lei, H.; Jia, X.; Mao, C.; Ruan, L.; Zhou, X.; Wang, Z.; Chen, F.; Chen, W. Tribo-Catalytic Degradation of Methyl Orange Solutions Enhanced by Silicon Single Crystals. *Coatings* **2023**, *13*, 1804. <https://doi.org/10.3390/coatings13101804>

Academic Editor: Alessandro Latini

Received: 21 September 2023

Revised: 17 October 2023

Accepted: 18 October 2023

Published: 20 October 2023



**Copyright:** © 2023 by the authors. Licensee MDPI, Basel, Switzerland. This article is an open access article distributed under the terms and conditions of the Creative Commons Attribution (CC BY) license (<https://creativecommons.org/licenses/by/4.0/>).

## 1. Introduction

The emergence of tribo-catalysis as a promising approach to address the crises of fossil energy shortage and environmental pollution has captured the attention of many researchers [1–7]. Most current related research works utilize a standard or modified magnetic stirring system, where frictions between the magnetic rotation section, catalyst, and the bottom of the container play a critical role in converting mechanical energy to chemical energy [8–13]. Mechanical energy has been harnessed through friction for applications such as hydrogen generation, dye degradation [14–17], toxins degradation [18], and CO<sub>2</sub> reduction [19,20].

To boost the efficiency of tribo-catalysis in various applications, numerous studies have been conducted in recent years, which can be broadly categorized into two groups. In the first group, investigations are focused on some specific aspects of catalysts in tribo-catalysis,

including the synthesis of particles with particular morphologies [9,11,21,22], the modulation of electronic structure [8,18,23,24], and the construction of heterojunctions [10,25]. The other group pays considerable attention to regulating friction pairs in tribo-catalysis. Rao et al. found that after 8 h of magnetic stirring, the degradation efficiencies of Rhodamine B (RhB) solution by BaTiO<sub>3</sub> nanoparticles were 88%, 94.7%, and 99.1% for the friction pairs of glass beaker-PTFE bar, PP beaker-PTFE bar, and PTFE beaker-PTFE bar, respectively [23]. Dong et al. discovered that the degradation efficiency of RHB or 2,4-DCP by BiWO<sub>3</sub> is significantly improved by adding PP or PTFE particles to form new friction pairs with BiWO<sub>3</sub> [26]. In our recent paper on the tribo-catalytic conversion of H<sub>2</sub>O and CO<sub>2</sub> by NiO particles, we found that the production of CH<sub>4</sub> increased to 7 and 5 folds when PVC and stainless steel 316 were coated on the reactor bottom, respectively [27]. In another latest paper on the tribo-catalytic conversion of H<sub>2</sub>O and CO<sub>2</sub> by Co<sub>3</sub>O<sub>4</sub> nanoparticles, the amounts of H<sub>2</sub> and CH<sub>4</sub> increased by 2 and 26 folds, respectively, through coating Ti on the glass reactor bottom [28]. Similarly, for tribo-catalytic conversion of H<sub>2</sub>O and CO<sub>2</sub> using a copper magnetic rotary disk, the production of flammable gases also obviously changed while coating Al<sub>2</sub>O<sub>3</sub>, copper, or titanium on reactor bottoms [29]. Regulating friction pair is especially effective in boosting tribo-catalysis efficiency, and coating certain materials on container bottoms is a straightforward method to realize it.

To date, two distinct mechanisms have been proposed for tribo-catalysis—electron transfer across atoms and electron transition [30]. In the former, electrons are transferred between materials through friction, and materials that gain or lose electrons generate active species to initiate subsequent redox reactions. In the latter, electron-hole pairs are excited in a material by mechanical energy absorbed through friction, which then results in redox reactions in the surrounding environments, similar to what happens in photo-catalysis. It is well-known that silicon is the most abundant element in Earth's crust. It is cost-effective, possesses a narrow band gap, and exhibits excellent processing performance, making it widely adopted in photovoltaic applications to convert solar energy into electricity. According to the second mechanism for tribo-catalysis, the generation of electrons and holes in a material by mechanical energy is primarily determined by its energy band structure. The purpose of this work is to explore tribo-catalysis by materials with narrow band gaps. Given that silicon is a typical semiconductor with a narrow band gap, we coated silicon single crystals on the bottoms of glass beakers, where some organic dyes were degraded by oxide particles through magnetic stirring. With such silicon single crystal coatings, 30 mg/L methyl orange (MO) solutions were found to be quickly de-colored, even by alumina particles, under magnetic stirring. MO is famous for the presence of high-energy bonds (C=N, N=N) in its molecules, and such a concentrated MO solution is difficult to degrade through a conventional catalytic method [31–33].

## 2. Materials and Methods

### 2.1. Materials Information

Silicon (110) single crystal wafers ( $\rho > 10^5 \Omega \cdot \text{cm}$ ) with a diameter of 40 mm and a thickness of 0.5 mm were purchased from Hangzhou Jingxin Electronic Technology Co., Hangzhou, China. High-purity  $\alpha$ -Al<sub>2</sub>O<sub>3</sub> nanoparticles (99.9 wt%, average particle size: 150–500 nm) were obtained from XFNANO Materials Tech. Co., Ltd., Nanjing, China, and  $\alpha$ -Al<sub>2</sub>O<sub>3</sub> laminated powder was purchased from Naiou Nano Technology Co., Shanghai, China.

### 2.2. Coating Silicon Single Crystal Wafers on the Bottoms of Glass Beakers

For some commercial flat-bottomed glass beakers of  $\phi$  45 mm  $\times$  60 mm, silicon (110) single crystal wafers of  $\phi$  40 mm  $\times$  0.5 mm were first coated on their bottoms through a glue. In this way, flat-bottomed glass beakers with both glass and Si-coated bottoms were available separately for further investigations.

### 2.3. Tribo-Catalytic Degradation of MO Solutions in Glass Beakers

In a typical experiment, 300 mg of  $\alpha$ -Al<sub>2</sub>O<sub>3</sub> was dispersed in 30 mL of 30 mg/L MO aqueous solution in a glass beaker. The suspension was magnetically stirred using a homemade PTFE magnetic rotary disk at 400 rpm in the dark at room temperature (25 °C). The details of the PTFE magnetic rotary disk were described in previous work [15]. During the tribo-catalytic process, 1 mL of the solution was taken out every 30 min, followed by centrifugal separation to obtain the supernatant. The concentration of MO was measured by recording the absorption spectra using a Shimadzu 2550 UV-Vis spectrometer (UV-2550; Shimadzu, Kyoto, Japan) over a 200–800 nm range.

### 2.4. Analyses of Degradation Products of MO through a Mass Spectrometer

The products resulting from the tribo-catalytic degradation of MO solutions in Si-coated beakers were further analyzed using a mass spectrometer Thermo Q-Exactive Plus (Thermo Scientific, San Jose, CA, USA) equipped with a heated electrospray ionization (HESI) source with the mass scan range set to  $m/z$  60–350. The mobile phases used in the analysis were acetonitrile and 0.01 mol/L acetic acid.

### 2.5. Detection of Radical Species

Electron paramagnetic resonance (EPR) spectroscopy was employed to probe the reactive oxygen species of  $\bullet$ OH and  $\bullet$ O<sub>2</sub><sup>−</sup>, which are essential in attacking dye macromolecules during the catalytic process of dye degradation. In a Si-coated flat-bottomed beaker, 0.15 g of Al<sub>2</sub>O<sub>3</sub> nanoparticles and 50  $\mu$ L of 5,5-Dimethyl-1-pyrroline N-oxide (DMPO) were added to 10 mL of deionized water for the detection of hydroxyl radical production; 0.15 g of Al<sub>2</sub>O<sub>3</sub> nanoparticles and 50  $\mu$ L of 5,5-Dimethyl-1-pyrroline N-oxide (DMPO) were added to 10 mL of methanol for the detection of superoxide radical production. The same experimental conditions were followed to detect  $\bullet$ OH and  $\bullet$ O<sub>2</sub><sup>−</sup> without Al<sub>2</sub>O<sub>3</sub> nanoparticles. Magnetic stirring was carried out using a PTFE magnetic rotary disk at 400 rpm for 30 min at room temperature without light. EPR spectra were recorded on a Bruker A300 paramagnetic resonance spectrometer.

## 3. Results and Discussion

The influence of silicon single crystals on tribo-catalytic degradation of various organic dyes employing different catalysts has been thoroughly explored. The tribo-catalytic degradation of 30 mg/L MO aqueous solutions by Al<sub>2</sub>O<sub>3</sub> powders in Si-coated glass beakers has drawn our attention for two compelling reasons. Firstly, Al<sub>2</sub>O<sub>3</sub> is well recognized for its wide band gap, and the excitation of electron-hole pairs through mechanical energy can be attributed to silicon only when it interacts with Al<sub>2</sub>O<sub>3</sub> through friction. Secondly, owing to the presence of azo double bonds in its molecular structure, MO, especially at a high concentration of 30 mg/L, poses a challenging target for degradation. This demonstrates the potential of silicon in tribo-catalysis.

In this study, two types of  $\alpha$ -Al<sub>2</sub>O<sub>3</sub> white powders were analyzed using a scanning electron microscope (Zeiss GeminiSEM 500, Jena, Germany), and their SEM images are presented in Figure 1. For the  $\alpha$ -Al<sub>2</sub>O<sub>3</sub> nanoparticles, referred to as Al<sub>2</sub>O<sub>3</sub> I hereafter, the particles appear as irregular polyhedrons ranging from 200 to 500 nm, as depicted in Figure 1a. In contrast, the  $\alpha$ -Al<sub>2</sub>O<sub>3</sub> laminated powder (Al<sub>2</sub>O<sub>3</sub> II) consists of laminate-like particles as large as 5  $\mu$ m, as shown in Figure 1b. The two kinds of  $\alpha$ -Al<sub>2</sub>O<sub>3</sub> white powders differ greatly in both size and shape.

For reference, Figure 2a displays the UV-visible absorption spectrums of a 30 mg/L MO solution during magnetic stirring with Al<sub>2</sub>O<sub>3</sub> I activated by a Teflon magnetic rotary disk in a glass beaker. No discernible change was observed in the absorption spectrum, even after 150 min of magnetic stirring. This observation aligns with the fact that degrading a 30 mg/L MO solution is exceptionally challenging, as described above. In stark contrast, an entirely different outcome was observed when a 30 mg/L MO solution, suspended with Al<sub>2</sub>O<sub>3</sub> I, was magnetically stirred in a Si-coated beaker. As illustrated in Figure 2b,

the absorption peak at 450 nm completely disappeared after 120 min of magnetic stirring. Concurrently, an obvious color change, from yellow to colorless, was observed for the solution, as indicated in the inset. When  $\text{Al}_2\text{O}_3$  I was replaced with  $\text{Al}_2\text{O}_3$  II, a similar result was obtained, albeit with slower changes in absorption peak and dye color, as demonstrated in Figure 2c. Conversely, when the solution lacked suspended particles, no observable alterations occurred when the solution was magnetically stirred in a Si-coated beaker, as shown in Figure 2d. Obviously, the friction between  $\text{Al}_2\text{O}_3$  and silicon was pivotal in the observed degradation.

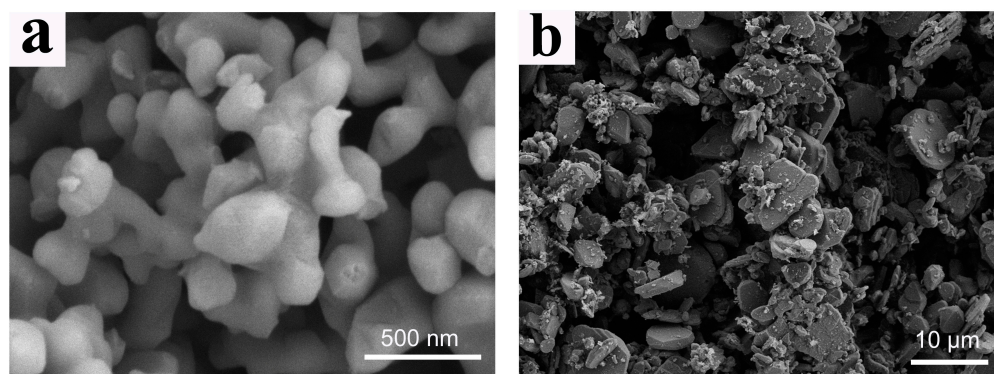


**Figure 1.** SEM images of  $\text{Al}_2\text{O}_3$  powders used in this study: (a)  $\alpha\text{-Al}_2\text{O}_3$  nanoparticles, termed as  $\text{Al}_2\text{O}_3$  I; (b)  $\alpha\text{-Al}_2\text{O}_3$  laminated powder, termed as  $\text{Al}_2\text{O}_3$  II.

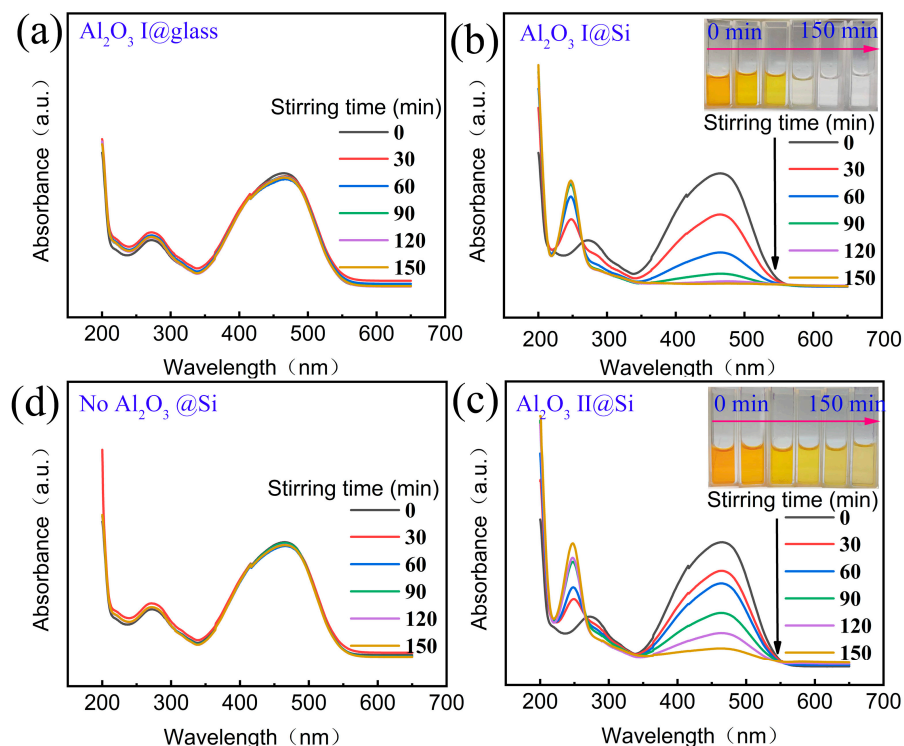


**Figure 2.** UV-Vis adsorption spectra and color evolution for a 30 mg/L MO solution in the course of magnetic stirring: (a) suspended with  $\text{Al}_2\text{O}_3$  I in a glass beaker; (b) suspended with  $\text{Al}_2\text{O}_3$  I in a Si-coated beaker; (c) suspended with  $\text{Al}_2\text{O}_3$  II in a Si-coated beaker; (d) with no particles suspended in a Si-coated beaker.

However, it is worth pointing out that a new peak at 250 nm in the UV region appeared when the peak at 450 nm disappeared in the UV-Vis adsorption spectra presented in Figure 2b,c. A similar phenomenon had been observed in the context of photocatalytic degradation of MO, where it was suggested that MO molecules were broken into small

molecules of some byproducts [34–36]. Mass spectrometry tests were performed to identify the byproducts obtained in this study. A 30 mL solution of 30 mg/L MO, suspended with 300 mg of Al<sub>2</sub>O<sub>3</sub> I, was magnetically stirred using a Teflon magnetic rotary disk at 400 rpm in a Si-coated glass beaker at 25 °C in darkness. Samples were extracted separately from the original MO solution, after 90 and 240 min of magnetic stirring, for mass spectrometry analyses. The outcomes of these analyses are presented in Figure 3. In Figure 3a, a prominent mass spectral peak at  $m/z = 304$  is evident for the original MO solution, corresponding to the ionization of the methyl orange parent molecule. As the stirring time reached 90 min, the intensity of the absorption peak at  $m/z = 304$  declined by at least half. Simultaneously, new peaks emerged at  $m/z = 150$ ,  $m/z = 122$ ,  $m/z = 118$ , and  $m/z = 109$ , representing intermediates in the degradation process of methyl orange molecule. After 240 min of stirring, the peak at  $m/z = 304$  disappeared, and the MZ signals of those intermediate products exhibited a slight decrease.

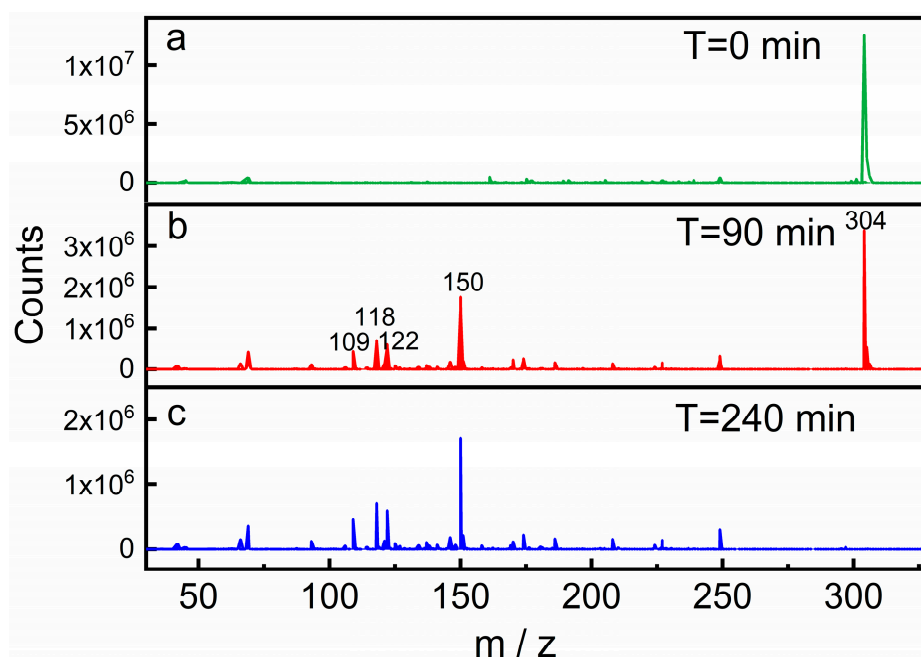


**Figure 3.** Mass spectrums: (a) original 30 mg/L MO solution; (b) after 90 min of magnetic stirring; (c) after 240 min of magnetic stirring with Al<sub>2</sub>O<sub>3</sub> I in a Si-coated beaker.

The addition of •OH radicals to the azo double bond has been proposed as the initial step in the oxidative bond cleavages for azo dyes [37–39]. This process is believed to account for the variation from  $m/z = 304$  to  $m/z = 150$  (nitro-*so*-N,N-dimethylaniline) observed in the ion mass spectrums in this study, and the possible destruction process is depicted in Figure 4a. Three major degradation byproducts are displayed in Figure 4b, with  $m/z = 122$  corresponding to benzoic acid [40],  $m/z = 118$  to succinic acid [41], and  $m/z = 109$  to *p*-phenol [42]. Clearly, the degradation observed in this study is a partial degradation and it remains a challenge to degrade concentrated MO solutions into non-toxic and harmless water and CO<sub>2</sub>.

It is worth noting that there were no observable changes in either Al<sub>2</sub>O<sub>3</sub> I or Al<sub>2</sub>O<sub>3</sub> II morphology after undergoing extended magnetic stirring for dozens of hours. Since silicon is considerably softer than Al<sub>2</sub>O<sub>3</sub>, inspecting the surface of silicon single crystals after friction with Al<sub>2</sub>O<sub>3</sub> during magnetic stirring is imperative. In Figure 5a, an optical microscope image illustrates the surface of an as-received silicon single crystal, which appears exceptionally smooth with minimal defects. Conversely, Figure 5b reveals that some scratches 1–2 μm wide were observed on the surface of a silicon single crystal after being treated as a coating through 10 h of magnetic stirring with Al<sub>2</sub>O<sub>3</sub> I. Despite these scratches, the successful degradation of methyl orange was repeated in a beaker coated

with this silicon single crystal, indicating that these surface imperfections had no adverse effect on subsequent catalytic utilization.

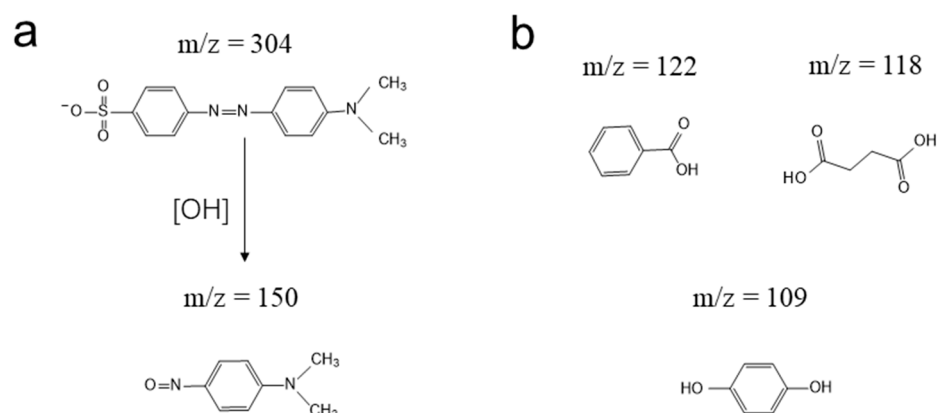


**Figure 4.** (a) Attack of  $\bullet\text{OH}$  radicals to the azo double bond; (b) Structural formulas for three main byproducts, to which methyl orange is converted.

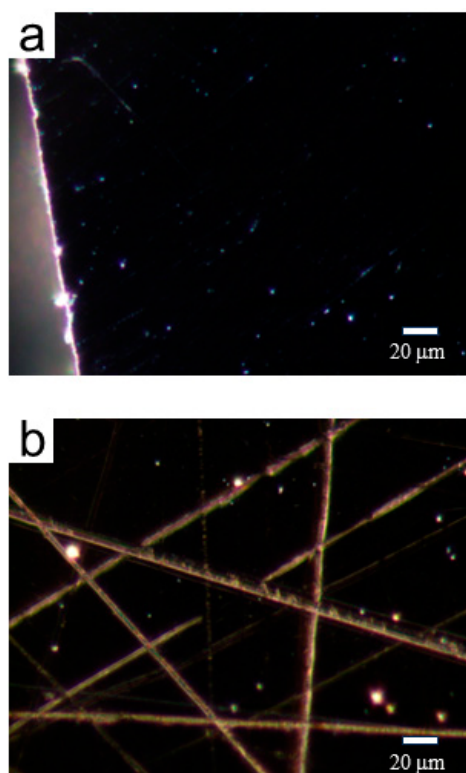


**Figure 5.** Optical microscope image for the surface of: (a) an as-received single crystal silicon; (b) a silicon single crystal after being treated as a coating through magnetic stirring with  $\text{Al}_2\text{O}_3$  I for 10 h.

In catalytic applications, particular active radicals are formed first, which subsequently drive various specific reactions. The EPR spectra obtained in this study are shown in Figure 6. In a silicon-coated beaker containing a DMPO aqueous solution suspended with  $\text{Al}_2\text{O}_3$  I, an unmistakable characteristic peak corresponding to hydroxyl radicals (1:2:2:1) was observed in the EPR measurement after 30 min of magnetic stirring using a Teflon magnetic rotary disk, as shown in Figure 6a [43], while for methanol added with DMPO suspended with  $\text{Al}_2\text{O}_3$  I in a silicon-coated beaker, four characteristic peaks representing superoxide radicals appeared in a 1:1:1:1 ratio after 30 min of magnetic stirring, as illustrated in Figure 6b [44]. In contrast, no characteristic signals were detected in the two control experiments, with no  $\text{Al}_2\text{O}_3$  particles suspended in the solutions. These results

suggest that the generation of hydroxyl and superoxide radicals is a consequence of the friction between  $\text{Al}_2\text{O}_3$  and silicon in magnetic stirring. Regarding the disparity in MO degradation observed between  $\text{Al}_2\text{O}_3$  I and  $\text{Al}_2\text{O}_3$  II, it is likely attributed to the fact that  $\text{Al}_2\text{O}_3$  I, with its much smaller particles, forms more friction with silicon single crystals compared to  $\text{Al}_2\text{O}_3$  II when subjected to the same magnetic stirring conditions.

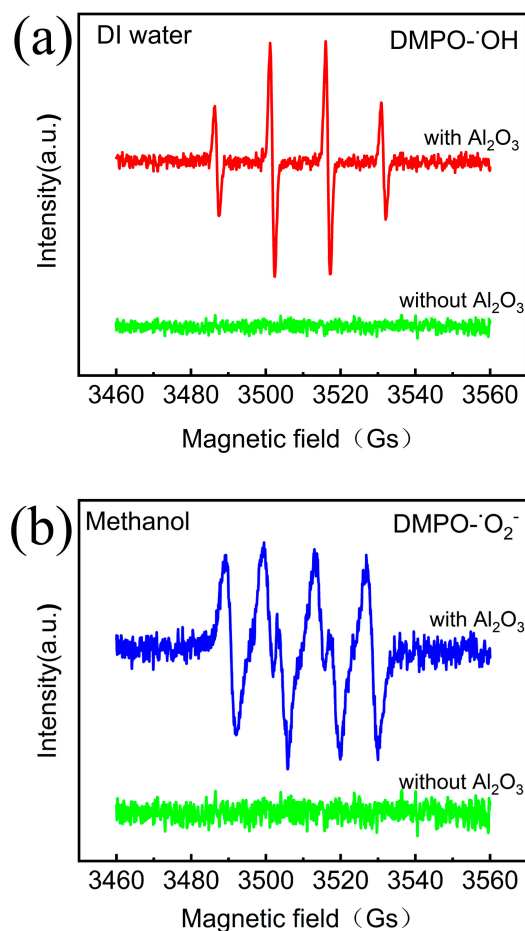


**Figure 6.** EPR spectra with DMPO as a spin-trap reagent were obtained for deionized water and methanol solution, where  $\text{Al}_2\text{O}_3$  nanoparticles were magnetically stirred using a Teflon magnetic rotary disk separately in a Si-coated beaker: (a) in deionized water, detecting hydroxyl radicals; (b) in methanol solution, detecting superoxide radicals.

In tribo-catalytic investigations, it is widely accepted that friction energy excites electron-hole pairs in materials during friction [45–47], which subsequently induces redox reactions in ambient environments. Given the degradation of MO solutions associated with silicon single crystals observed in this study, it is reasonable to assume that, through the friction between  $\text{Al}_2\text{O}_3$  particles and silicon single crystals in magnetic stirring, as shown in Figure 7, electron-hole pairs are excited in silicon:



Then, the electrons and holes diffuse into the ambient solutions, leading to the formation of some radicals and, ultimately, the degradation of the MO dye:





It is noteworthy that, in previous investigations of tribo-catalytic degradation of organic dyes, electron-hole pairs were consistently excited in particulate semiconductors by friction energy [5,15], which then diffused to the surfaces of the particles, inducing redox reactions in the ambient environment. This study marks the first instance where bulk semiconductors have electron-hole pairs excited through friction energy, instigating redox reactions in the ambient environment.

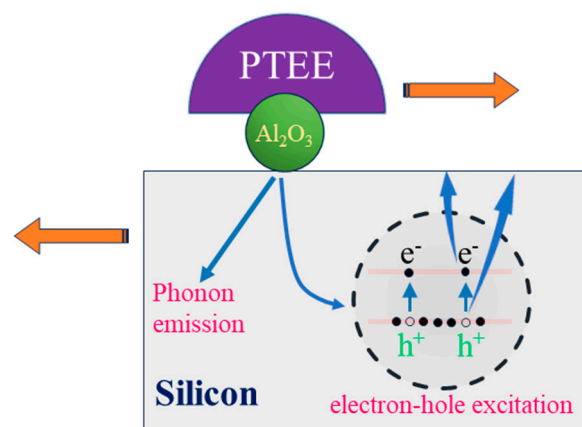


**Figure 7.** Mechanism diagram for the excitation of electron-hole pairs in silicon single crystals through the friction with  $\text{Al}_2\text{O}_3$  particles in magnetic stirring.

As previously described, MO solutions with concentrations as high as 30 mg/L have proven challenging to degrade through current catalytic technologies, including photocatalysis. The findings of this study thus underscore the potential of tribo-catalysis in harnessing mechanical energy for environmental remediation.

#### 4. Conclusions

An effect has been observed in the tribo-catalytic degradation of concentrated MO solutions when utilizing silicon single crystals as coatings. In glass beakers coated with silicon single crystals, 30 mg/L MO solutions suspended with alumina nanoparticles were changed from yellow to colorless within 120 min when Teflon magnetic rotary disks were driven to rotate at 400 rpm. Notably, the characteristic absorption peak of MO at 450 nm gradually weakened and eventually vanished, while a new absorption peak at 250 nm emerged in the UV-Vis spectrum over time. In-depth mass spectrometry tests further illuminated the degradation process, revealing that  $\bullet\text{OH}$  radicals initiated the breakdown of the nitrogen-nitrogen double bond within MO molecules. This process produced three major intermediate products: benzoic acid (with  $m/z = 122$ ), succinic acid ( $m/z = 118$ ), and p-phenol ( $m/z = 109$ ). Some comparison experiments have been conducted to show that the friction between silicon and alumina in magnetic stirring has resulted in the observed degradation, and hydroxyl and superoxide radicals have been detected to generate from the friction through EPR analysis. It is proposed that electron-hole pairs are excited in silicon single crystals due to the friction with alumina, which diffuse to the surface of the single crystals, resulting in redox reactions in an ambient environment. These results suggest the potential of using silicon in the tribo-catalytic degradation of concentrated MO solutions.

**Author Contributions:** Conceptualization, X.C. and W.C.; methodology, X.C., H.L., X.J. and C.M.; validation, X.Z., Z.W. and W.C.; formal analysis, X.C., H.L., X.J. and W.C.; investigation, X.C., Z.G., C.M. and L.R.; data curation, H.L.; writing—original draft preparation, X.C.; writing—review and editing, Z.G. and W.C.; visualization, H.L.; supervision, W.C.; project administration, Z.W., F.C. and W.C.; funding acquisition, Z.W. and F.C. All authors have read and agreed to the published version of the manuscript.

**Funding:** This research was funded by the National Key R&D Program of China under Grant No. 2023YFE0204400, and by the National Natural Science Foundation of China under Grant No. U2067207.

**Institutional Review Board Statement:** Not applicable.

**Informed Consent Statement:** Not applicable.

**Data Availability Statement:** The data underlying this article will be shared on reasonable request to the corresponding author.

**Conflicts of Interest:** The authors declare no conflict of interest.

## References

1. Ren, X.; Dong, L.; Xu, D.; Hu, B. Challenges towards hydrogen economy in China. *Int. J. Hydrogen Energy* **2020**, *45*, 34326–34345. [CrossRef]
2. Goldthau, A.; Tagliapietra, S. Energy crisis: Five questions that must be answered in 2023. *Nature* **2022**, *612*, 627–630. [CrossRef]
3. Zor, S. Conservation or revolution? The sustainable transition of textile and apparel firms under the environmental regulation: Evidence from China. *J. Clean. Prod.* **2023**, *382*, 135339. [CrossRef]
4. Singha, K.; Pandit, P.; Maity, S.; Sharma, S.R. Harmful environmental effects for textile chemical dyeing practice. In *Green Chemistry for Sustainable Textiles*; Ibrahim, N., Hussain, C.M., Eds.; Woodhead Publishing: Sawston, UK, 2021; pp. 153–164.
5. Li, P.; Wu, J.; Wu, Z.; Jia, Y.; Ma, J.; Chen, W.; Zhang, L.; Yang, J.; Liu, Y. Strong tribocatalytic dye decomposition through utilizing triboelectric energy of barium strontium titanate nanoparticles. *Nano Energy* **2019**, *63*, 103832. [CrossRef]
6. Fan, F.; Xie, S.; Wang, G.; Tian, Z. Tribocatalysis: Challenges and perspectives. *Sci. China Chem.* **2021**, *64*, 1609–1613. [CrossRef]
7. Tong, W.; An, Q.; Li, Y.; Li, X.; Zhang, Y. Weak-force energy development and its self-powered environmental purification. *Chin. Sci. Bull.* **2023**, *68*, 1381–1391. [CrossRef]
8. Yang, B.; Chen, H.; Yang, Y.; Wang, L.; Bian, J.; Liu, Q.; Lou, X. Insights into the tribo-/pyro-catalysis using Sr-doped BaTiO<sub>3</sub> ferroelectric nanocrystals for efficient water remediation. *Chem. Eng. J.* **2021**, *416*, 128986. [CrossRef]
9. Jin, Z.; Zheng, X.; Zhu, Z.; Hu, C.; Liu, L.; Fang, L.; Luo, N.; Cheng, Z. Enhanced triboelectric degradation of organics by tuning the synergy between ferroelectric polarization and illumination. *Mater. Today Chem.* **2023**, *29*, 101427. [CrossRef]
10. Jin, Z.; Zheng, X.; Zhu, Z.; Hu, C.; Liu, L.; Fang, L.; Cheng, Z. Enhanced triboelectric degradation of organics by regulating oxygen vacancies and constructing heterojunctions. *Appl. Surf. Sci.* **2023**, *625*, 157228. [CrossRef]
11. Xu, Y.; Yin, R.; Zhang, Y.; Zhou, B.; Sun, P.; Dong, X. Unveiling the mechanism of frictional catalysis in water by Bi<sub>12</sub>TiO<sub>20</sub>: A charge transfer and contaminant decomposition path study. *Langmuir* **2022**, *38*, 14153–14161. [CrossRef]
12. Yu, H.; Fu, J.; Zhu, X.; Zhao, Z.; Sui, X.; Sun, S.; He, X.; Zhang, Y.; Ye, W. Tribocatalytic degradation of organic pollutants using Fe<sub>2</sub>O<sub>3</sub> nanoparticles. *ACS Appl. Nano Mater.* **2023**, *6*, 14364–14373. [CrossRef]
13. Wu, M.; Xu, Y.; He, Q.; Sun, P.; Weng, X.; Dong, X. Tribocatalysis of homogeneous material with multi-size granular distribution for degradation of organic pollutants. *J. Colloid Interface Sci.* **2022**, *622*, 602–611. [CrossRef] [PubMed]
14. Zhao, J.; Chen, L.; Luo, W.; Li, H.; Wu, Z.; Xu, Z.; Zhang, Y.; Zhang, H.; Yuan, G.; Gao, J. Strong tribo-catalysis of zinc oxide nanorods via triboelectrically-harvesting friction energy. *Ceram. Int.* **2020**, *46*, 25293–25298. [CrossRef]
15. Cui, X.; Li, P.; Lei, H.; Tu, C.; Wang, D.; Wang, Z.; Chen, W. Greatly enhanced tribocatalytic degradation of organic pollutants by TiO<sub>2</sub> nanoparticles through efficiently harvesting mechanical energy. *Sep. Purif. Technol.* **2022**, *289*, 120814. [CrossRef]
16. Sun, C.; Guo, X.; Ji, R.; Hu, C.; Liu, L.; Fang, L.; Cheng, Z.; Luo, N. Strong tribocatalytic dye degradation by tungsten bronze Ba<sub>4</sub>Nd<sub>2</sub>Fe<sub>2</sub>Nb<sub>8</sub>O<sub>30</sub>. *Ceram. Int.* **2021**, *47*, 5038–5043. [CrossRef]
17. Sun, C.; Guo, X.; Hu, C.; Liu, L.; Fang, L.; Cheng, Z.; Luo, N. Tribocatalytic degradation of dyes by tungsten bronze ferroelectric Ba<sub>2.5</sub>Sr<sub>2.5</sub>Nb<sub>8</sub>Ta<sub>2</sub>O<sub>30</sub> submicron particles. *RSC Adv.* **2021**, *11*, 13386–13395. [CrossRef] [PubMed]
18. Hu, J.; Ma, W.; Pan, Y.; Cheng, Z.; Yu, S.; Gao, J.; Zhang, Z.; Wan, C.; Qiu, C. Insights on the mechanism of Fe doped ZnO for tightly-bound extracellular polymeric substances tribo-catalytic degradation: The role of hydration layers at the interface. *Chemosphere* **2021**, *276*, 130170. [CrossRef]
19. Li, P.; Tang, C.; Xiao, X.; Jia, Y.; Chen, W. Flammable gases produced by TiO<sub>2</sub> nanoparticles under magnetic stirring in water. *Friction* **2022**, *10*, 1127–1133. [CrossRef]
20. Li, P.; Tang, C.; Chen, L.; Hu, Y.; Xiao, X.; Chen, W. Reduction of CO<sub>2</sub> by TiO<sub>2</sub> nanoparticles through friction in water. *Acta Phys. Sin.* **2021**, *70*, 214601. [CrossRef]
21. Yang, B.; Chen, H.; Guo, X.; Wang, L.; Xu, T.; Bian, J.; Yang, Y.; Liu, Q.; Du, Y.; Lou, X. Enhanced tribocatalytic degradation using piezoelectric CdS nanowires for efficient water remediation. *J. Mater. Chem. C* **2020**, *8*, 14845–14854. [CrossRef]
22. Zhang, Q.; Jia, Y.; Wang, X.; Zhang, L.; Yuan, G.; Wu, Z. Efficient tribocatalysis of magnetically recyclable cobalt ferrite nanoparticles through harvesting friction energy. *Sep. Purif. Technol.* **2023**, *307*, 122846. [CrossRef]
23. Liu, S.; Yang, Y.; Hu, Y.; Rao, W. Effect of strontium substitution on the tribocatalytic performance of barium titanate. *Materials* **2023**, *16*, 3160. [CrossRef] [PubMed]

24. Tang, Q.; Zhu, M.; Zhang, H.; Gao, J.; Kwok, K.W.; Kong, L.; Jia, Y.; Liu, L.; Peng, B. Enhanced tribocatalytic degradation of dye pollutants through governing the charge accumulations on the surface of ferroelectric barium zirconium titanate particles. *Nano Energy* **2022**, *100*, 107519. [[CrossRef](#)]
25. Li, X.; Wang, J.; Zhang, J.; Zhao, C.; Wu, Y.; He, Y. Cadmium sulfide modified zinc oxide heterojunction harvesting ultrasonic mechanical energy for efficient decomposition of dye wastewater. *J. Colloid Interface Sci.* **2022**, *607*, 412–422. [[CrossRef](#)] [[PubMed](#)]
26. Wu, M.; Zhang, Y.; Yi, Y.; Zhou, B.; Sun, P.; Dong, X. Regulation of friction pair to promote conversion of mechanical energy to chemical energy on Bi<sub>2</sub>WO<sub>6</sub> and realization of enhanced tribocatalytic activity to degrade different pollutants. *J. Hazard. Mater.* **2023**, *459*, 132147. [[CrossRef](#)] [[PubMed](#)]
27. Lei, H.; Jia, X.; Wang, H.; Cui, X.; Jia, Y.; Fei, L.; Chen, W. Tribo-catalytic conversions of H<sub>2</sub>O and CO<sub>2</sub> by NiO particles in reactors with plastic and metallic coatings. *Coatings* **2023**, *13*, 396. [[CrossRef](#)]
28. Jia, X.; Wang, H.; Lei, H.; Mao, C.; Cui, X.; Liu, Y.; Jia, Y.; Yao, W.; Chen, W. Boosting tribo-catalytic conversion of H<sub>2</sub>O and CO<sub>2</sub> by Co<sub>3</sub>O<sub>4</sub> nanoparticles through metallic coatings in reactors. *J. Adv. Ceram.* **2023**. [[CrossRef](#)]
29. Cui, X.; Wang, H.; Lei, H.; Jia, X.; Jiang, Y.; Fei, L.; Jia, Y.; Chen, W. Surprising tribo-catalytic conversion of H<sub>2</sub>O and CO<sub>2</sub> into flammable gases utilizing frictions of copper in Water. *ChemistrySelect* **2023**, *8*, e202204146. [[CrossRef](#)]
30. Li, X.; Tong, W.; Shi, J.; Chen, Y.; Zhang, Y.; An, Q. Tribocatalysis mechanisms: Electron transfer and transition. *J. Mater. Chem. A* **2023**, *11*, 4458–4472. [[CrossRef](#)]
31. Zhai, L.; Bai, Z.; Zhu, Y.; Wang, B.; Luo, W. Fabrication of chitosan microspheres for efficient adsorption of methyl orange. *Chin. J. Chem. Eng.* **2018**, *26*, 657–666. [[CrossRef](#)]
32. Sanromán, M.Á.; Pazos, M.; Camele, C. Optimisation of electrochemical decolourisation process of an azo dye, methyl orange. *J. Chem. Technol. Biotechnol.* **2004**, *79*, 1349–1353. [[CrossRef](#)]
33. Liu, T.; Wang, L.; Lu, X.; Fan, J.; Cai, X.; Gao, B.; Miao, R.; Wang, J.; Lv, Y. Comparative study of the photocatalytic performance for the degradation of different dyes by ZnIn<sub>2</sub>S<sub>4</sub>: Adsorption, active species, and pathways. *RSC Adv.* **2017**, *7*, 12292–12300. [[CrossRef](#)]
34. Li, X.; Zhu, J.; Li, H. Comparative study on the mechanism in photocatalytic degradation of different-type organic dyes on SnS<sub>2</sub> and CdS. *Appl. Catal. B Environ.* **2012**, *123*, 174–181. [[CrossRef](#)]
35. Wang, M.; Li, M.; Xu, L.; Wang, L.; Ju, Z.; Li, G.; Qian, Y. High yield synthesis of novel boron nitride submicro-boxes and their photocatalytic application under visible light irradiation. *Catal. Sci. Technol.* **2011**, *1*, 1159–1165. [[CrossRef](#)]
36. Filice, S.; D'Angelo, D.; Libertino, S.; Nicotera, I.; Kosma, V.; Privitera, V.; Scalese, S. Graphene oxide and titania hybrid nafion membranes for efficient removal of methyl orange dye from water. *Carbon* **2015**, *82*, 489–499. [[CrossRef](#)]
37. Joseph, J.M.; Destailats, H.; Hung, H.M.; Hoffmann, M.R. The sonochemical degradation of azobenzene and related azo dyes: Rate enhancements via Fenton's reactions. *J. Phys. Chem. A* **2000**, *104*, 301–307. [[CrossRef](#)]
38. Wojnárovits, L.; Takács, E. Irradiation treatment of azo dye containing wastewater: An overview. *Radiat. Phys. Sonochem.* **2008**, *77*, 225–244. [[CrossRef](#)]
39. Okitsu, K.; Iwasaki, K.; Yobiko, Y.; Bandow, H.; Nishimura, R.; Maeda, Y. Sonochemical degradation of azo dyes in aqueous solution: A new heterogeneous kinetics model taking into account the local concentration of OH radicals and azo dyes. *Ultrason. Sonochem.* **2005**, *12*, 255–262. [[CrossRef](#)]
40. Ariyanti, D.; Maillot, M.; Gao, W. Photo-assisted degradation of dyes in a binary system using TiO<sub>2</sub> under simulated solar radiation. *J. Environ. Chem. Eng.* **2018**, *6*, 539–548. [[CrossRef](#)]
41. Panda, N.; Sahoo, H.; Mohapatra, S. Decolourization of methyl orange using Fenton-like mesoporous Fe<sub>2</sub>O<sub>3</sub>-SiO<sub>2</sub> composite. *J. Hazard. Mater.* **2011**, *185*, 359–365. [[CrossRef](#)]
42. Khan, M.A.; Mutahir, S.; Wang, F.; Lei, W.; Xia, M.; Zhu, S. Facile one-step economical methodology of metal free g-C<sub>3</sub>N<sub>4</sub> synthesis with remarkable photocatalytic performance under visible light to degrade trans-resveratrol. *J. Hazard. Mater.* **2019**, *367*, 293–303. [[CrossRef](#)]
43. Lin, F.; Zhang, Y.; Wang, L.; Zhang, Y.; Wang, D.; Yang, M.; Yang, J.; Zhang, B.; Jiang, Z.; Li, C. Highly efficient photocatalytic oxidation of sulfur-containing organic compounds and dyes on TiO<sub>2</sub> with dual cocatalysts Pt and RuO<sub>2</sub>. *Appl. Catal. B Environ.* **2012**, *127*, 363–370. [[CrossRef](#)]
44. Duan, Y.; Luo, J.; Zhou, S.; Mao, X.; Shah, M.W.; Wang, F.; Chen, Z.; Wang, C. TiO<sub>2</sub>-supported Ag nanoclusters with enhanced visible light activity for the photocatalytic removal of NO. *Appl. Catal. B Environ.* **2018**, *234*, 206–212. [[CrossRef](#)]
45. Geng, L.; Qian, Y.; Song, W.; Bao, L. Enhanced tribocatalytic pollutant degradation through tuning oxygen vacancy in BaTiO<sub>3</sub> nanoparticles. *Appl. Surf. Sci.* **2023**, *637*, 157960. [[CrossRef](#)]
46. Schwab, T.; Thomele, D.; Aicher, K.; Dunlop, J.W.; McKenna, K.; Diwald, O. Rubbing powders: Direct spectroscopic observation of triboinduced oxygen radical formation in MgO nanocube ensembles. *J. Phys. Chem. C* **2021**, *125*, 22239–22248. [[CrossRef](#)] [[PubMed](#)]
47. Alabbad, E.A.; Bashir, S.; Liu, J.L. Efficient removal of direct yellow dye using chitosan crosslinked isovanillin derivative biopolymer utilizing triboelectric energy produced from homogeneous catalysis. *Catal. Today* **2022**, *400*, 132–145. [[CrossRef](#)]

**Disclaimer/Publisher's Note:** The statements, opinions and data contained in all publications are solely those of the individual author(s) and contributor(s) and not of MDPI and/or the editor(s). MDPI and/or the editor(s) disclaim responsibility for any injury to people or property resulting from any ideas, methods, instructions or products referred to in the content.